Evaluation of the Inertial Response of Variable-Speed Wind Turbines Using Advanced Simulation

Preprint

Xiao Wang, Jianhui Wang
Northeastern University, Shenyang, China

Wenzhong Gao, Weihang Yan
University of Denver

Eduard Muljadi, Vahan Gevorgian, Andrew Scholbrock
National Renewable Energy Laboratory

Presented at The Institute of Electrical and Electronics Engineers' Power & Energy Society General Meeting
Chicago, Illinois
July 16–20, 2017

NREL is a national laboratory of the U.S. Department of Energy
Office of Energy Efficiency & Renewable Energy
Operated by the Alliance for Sustainable Energy, LLC

This report is available at no cost from the National Renewable Energy Laboratory (NREL) at www.nrel.gov/publications.

Conference Paper
NREL/CP-5000-68073
August 2017

Contract No. DE-AC36-08GO28308

NOTICE

This report is available at no cost from the National Renewable Energy Laboratory (NREL) at www.nrel.gov/publications.

Available electronically at SciTech Connect http:/www.osti.gov/scitech

Available for a processing fee to U.S. Department of Energy and its contractors, in paper, from:

U.S. Department of Energy
Office of Scientific and Technical Information
P.O. Box 62
Oak Ridge, TN 37831-0062
OSTI http://www.osti.gov
Phone: 865.576.8401
Fax: 865.576.5728
Email: reports@osti.gov

Available for sale to the public, in paper, from:

U.S. Department of Commerce
National Technical Information Service
5301 Shawnee Road
Alexandria, VA 22312
NTIS http://www.ntis.gov
Phone: 800.553.6847 or 703.605.6000
Fax: 703.605.6900
Email: orders@ntis.gov

Cover Photos by Dennis Schroeder: (left to right) NREL 26173, NREL 18302, NREL 19758, NREL 29642, NREL 19795.

NREL prints on paper that contains recycled content.

Evaluation of the Inertial Response of Variable-Speed Wind Turbines Using Advanced Simulation

Xiao Wang, *Student Member, IEEE*, Wenzhong Gao, *Senior Member, IEEE*, Weihang Yan, Jianhui Wang, Eduard Muljadi, *Fellow, IEEE*, Vahan Gevorgian, *Member, IEEE,* Andrew Scholbrock

***Abstract*—In this paper, we focus on the temporary frequency support effect provided by wind turbine generators (WTGs) through the inertial response. With the implemented inertial control methods, the WTG is capable of increasing its active power output by releasing parts of the stored kinetic energy when the frequency excursion occurs. The active power can be boosted temporarily above the maximum power points, but the rotor speed deceleration follows and an active power output deficiency occurs during the restoration of rotor kinetic energy.**

In this paper, we evaluate and compare the inertial response induced by two distinct inertial control methods using advanced simulation. In the first stage, the proposed inertial control methods are analyzed in offline simulation. Using an advanced wind turbine simulation program, FAST with TurbSim, the response of the researched wind turbine is comprehensively evaluated under turbulent wind conditions, and the impact on the turbine mechanical components are assessed. In the second stage, the inertial control is deployed on a real 600-kW wind turbine, the three-bladed Controls Advanced Research Turbine, which further verifies the inertial control through a hardware-in-the-loop simulation. Various inertial control methods can be effectively evaluated based on the proposed two-stage simulation platform, which combines the offline simulation and real-time hardware-in-the-loop simulation. The simulation results also provide insights in designing inertial control for WTGs.

***Index Terms*—inertial response, WTG, frequency support, hardware-in-the-loop simulation, FAST.**

I. Introduction

Wind energy has experienced significant growth in recent decades, with the penetration level of wind power reaching as high as 50% in some areas of the United States [1], [2]. The application of affordable power electronics and advances in modern control enable sophisticated wind turbine design. Typically, a wind turbine is operated in a variable-speed mode as the extracted mechanical (aerodynamic) power can be maximized by keeping the optimal tip-speed ratio (TSR) in winds that are below the rated power of the wind turbine.

Difficulties arise for integration of large-scale wind power plants (WPPs) into the power grid. The frequency stability is a main concern of transmission system operators. Variable-speed wind turbines are equipped with power converters, making them partially or completely decoupled from the connected power system. Though the wind energy conversion system can be operated irrespective of the power system disturbances to some extent, the power system frequency stability is deteriorated because of the decreased inertial response and primary frequency regulation.

Transmission system operators revise their grid codes to accommodate the increased wind power integration. Large WPPs are required to provide frequency support similar to the inertial response of synchronous generators in North America [3]. Actually, the rotor speed range of a variable-speed WTG is larger than that of a synchronous generator, so they are capable of releasing more kinetic energy with the similar inertia constant; further, the released inertial power can be designed with flexible control methods, so the frequency support effect may be sustained longer [4], [5]. Various control methods have been developed to achieve the synthetic inertial response. The inertial control methods can be categorized into two types: frequency-based inertial control (FBIC), in which the rotor speed is regulated according to the rate of change of frequency (ROCOF) (or frequency deviation) in a similar manner to that of synchronous generators [6], [7], and step-wise inertial control (SIC), in which a variable-speed WTG is controlled to release a constant active power for a limited time duration [8], [9], with the shaped power reference commonly designed in the power-speed plane [4].

The aforementioned inertial control methods are evaluated and compared in this paper, and the wind turbine operation under highly turbulent wind conditions is emphasized. A two-stage simulation is carried out to evaluate the inertial control methods comprehensively: (1) the inertial response is tested using the advanced wind turbine simulation tools—FAST [10] and TurbSim [11]; (2) the hardware-in-the-loop (HIL) techniques are applied to test the

This work was supported in part by the U.S. Department of Energy under Contract No. DE-AC36-08-GO28308 with the National Renewable Energy Laboratory. Funding for the work was provided by the DOE Office of Energy Efficiency and Renewable Energy, Wind Energy Technologies Office.

X. Wang and J. Wang are with Northeastern University, Shenyang, China (e-mail: wangxiao.owl@gmail.com)

W. Gao and W. Yan are with University of Denver, Denver, CO, USA (e-mail: wenzhong.gao@du.edu)

E. Muljadi, V. Gevorgian, and Andrew Scholbrock are with the National Renewable Energy Laboratory, Golden, CO, USA (e-mail: eduard.muljadi@nrel.gov)

inertial response of a real 600-kW wind turbine—the three-bladed Controls Advanced Research Turbine (CART3), located at the National Wind Technology Center. The interface between LabVIEW (CART3 supervisory control and data acquisition [SCADA] system) and Simulink results in an effective testing procedure in that the developed inertial controllers in Simulink can be compiled and embedded into LabVIEW to control the CART3 directly, and the inertial controller will be simulated and modified further based on the response of the real wind turbine. The Western System Coordinating Council (WSCC) nine bus power system is modeled in Matlab/Simulink and a real-time digital simulator (RTDS) to test the inertial response of the aggregated WPP. The contribution of this work is developing a simulation platform to effectively evaluate different inertial control methods, and insights in designing inertial response for WTGs are provided.

II. Modeling and Control of a Variable-Speed WTG

There are two types of variable-speed WTGs: Type 3 doubly-fed induction generator (DFIG) or Type 4 permanent-magnet synchronous generator (PMSG) [12]. A Type 4 WTG consists of a full converter system interconnecting PMSG stator circuits and the point of common coupling. Compared to a DFIG WTG, a PMSG WTG is completely decoupled from the grid, and it is able to be driven directly by a wind turbine because of the multipoles structure; therefore, the gearbox, regarded as a vulnerable part, can be removed from a PMSG WTG. The expense of maintenance can be significantly reduced for a PMSG WTG because it is a rather tough and expensive task to fix the faults in the gearbox. These features lead to a higher efficiency and reliability of a PMSG WTG; however, the cost of the PMSG WTG is expected to be higher because of the full converter. Besides, the size of the direct-drive system is larger because of the multipoles structures. Even so, the PMSG WTG is increasing its market share along with the reduced price of power electronics, especially in the offshore wind market.

A. Basic Control Concepts for Variable-Speed Wind Turbines

Two control systems work together in a variable-speed WTG system [13]. A pitch controller regulates the pitch angle to restrict the rotor speed or mechanical power when the wind speed is above the rated value, which is also necessary to reduce the loads on the mechanical components of a wind turbine. When the rotor speed is below the rated value, it is controlled by the power converter system that is also in charge of the power injection of a WTG. The rotor speed is regulated in a way that maintains the optimal TSR to maximize the mechanical power extraction from the wind. The mechanical power is formulated in (1) [14], as:

$$P_m = \frac{1}{2}\rho\pi R^2 V_w^{\,3} C_p\left(\lambda, \beta\right) \tag{1}$$

The available mechanical power, P_m, relates to the power coefficient, C_p. It is determined by the TSR, λ, only when the pitch angle, β, is held constant. The parameters ρ, R, and V_w are the air density, rotor radius, and wind speed, respectively. The TSR is defined in (2), in which ω_r is the rotor speed.

$$\lambda = \frac{\omega_r R}{V_w} \tag{2}$$

The maximum power coefficient, $C_{p,\,max}$, corresponds to the optimal TSR and optimal pitch angle. Because of this, the rotor speed should be regulated proportionally to the wind speed to maximize the power extraction. However, tracking the optimal rotor speed tightly results in severe torque transients, and injects power oscillation due to the wind turbulence. Besides, it is difficult to measure the wind speed accurately across the whole rotor. As a result, it is more common to calculate the electromagnetic power or torque reference directly according to a predesigned lookup table. Because the optimal TSR, λ_{opt}, and $C_{p,\,max}$ are known in advance, the electromagnetic power reference is deduced as:

$$P_e = K\omega_r^{\,3} \tag{3}$$

where

$$K = \frac{1}{2}\rho\pi R^5 \frac{C_{p,\max}}{\lambda_{opt}^{\;3}} \tag{4}$$

In this method, the inertia of wind turbine rotating mass acts similar to an inductance in the electric circuit. The fluctuating power is smoothed and absorbed as the kinetic energy, instead of delivering to the grid directly, thereby improving the wind power quality [12].

B. FAST-Based CART3 Model

The CART3 is a 600-kW, three-bladed wind turbine at the National Wind Technology Center, located near Boulder, Colorado. This machine is specially designed for testing advanced control concepts with a customized and reprogrammable real-time controller and is equipped with numerous sensors for monitoring performance [15]. The CART3 employs a Type 4 WTG with a full converter system. Each blade can be independently pitched through its own servo system. As illustrated in Fig. 1, the CART3 is modeled based on FAST, which incorporates a simplified generator model, yaw controller, and pitch controller.

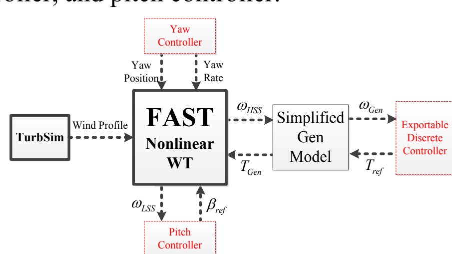

Fig. 1. Layout of the CART3 model using FAST and TurbSim

The exportable discrete controller employs the maximum power point tracking (MPPT) control in the baseline mode, and new control concepts can be implemented in it. The FAST-based nonlinear wind turbine can be operated under the stochastic, full field, turbulent wind speed profiles generated by TurbSim [11]. The wind turbulent intensity is a tunable setting in TurbSim; consequently, the researched wind turbine is evaluated with respect to various wind turbulence. After comprehensive case studies, the proposed control concept in the exportable discrete controller can be compiled and integrated into the CART3 SCADA system to control the real turbine, so new control concepts can be rapidly developed and tested based on the platform.

Power converters interface with the CART3 model and connected power system. In our previous work [16], the simplified generator in the CART3 model was fully replaced with a detailed PMSG and back-to-back average power converter to constitute a complete CART3-PMSG-integrated model. The PMSG and power converters can be either mathematical models or built-in blocks of SimPowerSystem in Simulink. However, it is difficult to simulate the power converters with pulse width modulation techniques in RTDS because of their high-frequency signals relative to the real-time simulation steps of RTDS [17]. Considering that renewable technologies, such as wind turbines and photovoltaics, are commonly interfaced with the grid via a current-controlled voltage source converter, a simplified converter model is employed here to integrate the wind turbine, as shown in Fig. 2.

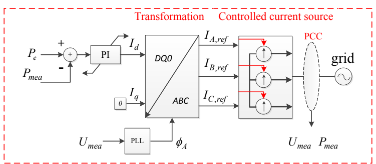

Figure 2. Simplified interface between the CART3 and the connected power system

III. Inertial control methods for variable-speed Wind Turbine Generators

As mentioned earlier, based on whether a frequency measurement exists or not, we divide inertial control methods into two distinct categories, each of which present different features for the frequency support.

A. Frequency-Based Inertial Control

The control logic for frequency-based inertial response is presented in Fig. 3. The filtered derivative of system frequency, df/dt, and frequency deviation, Δf, are multiplied by factors K_f and K_d, respectively. Then, this additional power is added to P_{MPPT} during the event of frequency excursion.

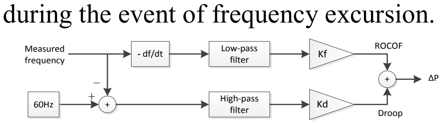

Figure 3. Simplified interface between the CART3 and the connected power system

A low-pass filter with a 0.1-s time constant is added to process the ROCOF signal. Therefore, the power or torque commands are smoothed to get rid of the severe transient loads caused by the noise. A high-pass filter with a 10-s time constant is added to the droop-based term so a constant frequency deviation cannot pass through and the WTG recovers automatically when the settling frequency is attained. The ROCOF-based term is dominant at the beginning of the frequency dip, whereas the frequency-deviation-based term is dominant when the frequency dip is arriving to the nadir, so the combination of the two parts provides a better response than a single one [18]. The scale factors, K_f and K_d, are used to strengthen the inertial response of each term.

B. Stepwise Inertial Control

The stepwise inertial control (SIC) method is capable of providing the maximum possible frequency support based on understanding the overproduction capability of variable-speed WTGs [9]. To protect the WTG system from damages, some restriction, such as the current and torque limit, must be maintained during the process of inertial response.

The SIC method implemented in this paper is an improved inertial control method, known as torque-limit-based inertial control (TLIC) [4]. The power reference of the inertial response is illustrated in Fig. 4. The power reference is defined in the deceleration (A-B-C trajectory) and acceleration (C-D-E-A trajectory) stages, respectively. When the frequency deviation is detected, the WTG output power will increase to Point B from the predisturbance Point A, and regulated along the B-C trajectory. The power reference at point B corresponds to the torque limit. In [4], the acceleration stage will be activated once the turbine settles at the quasi-stable point C, which is detected by monitoring if the rotor speed is nearly constant. Note that a small deloaded power is required at the beginning of the acceleration stage, and the constant power reference is maintained along D-E trajectory before the accelerating power reference meets the maximum power point tracking curve.

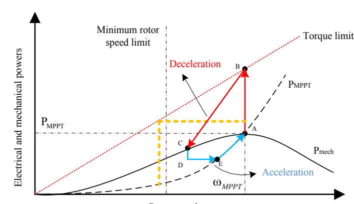

Figure 4. The improved SIC method— with TLIC in the power-speed plane.

However, the rotor speed will change a lot because of the turbulent wind speed, even when the mechanical torque and electromagnetic torque equals at point C. The assumption of the constant wind speed is rational only within a small time window, but it is not suitable for variable-speed wind turbines because the inertial response is much longer than that of conventional synchronous generators. As a result, the deceleration stage A-B-C is modified to be sustained for a predefined duration similar to that in a typical SIC method. Then, the acceleration stage is redesigned according to the control logics shown in Fig. 5. Instead of the constant power reference of DE, the accelerating power will decrease 0.08 p.u./s once the rotor speed is detected to decrease.

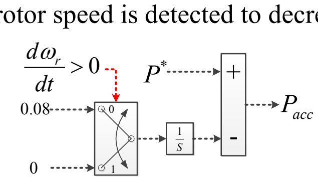

Figure 5. Control logics of accelerating the wind turbine in the modified TLIC method

The inertial control of a typical SIC method is illustrated in Fig. 4 by the yellow dashed line. By contrast, the inertial response may not be fully exploited with the predefined power increase, and overdeceleration may be observed when the rotor speed falls below the minimum rotor speed. Also, the secondary frequency dip may occur when the wind turbine decreases the active power output to restore the kinetic energy suddenly.

IV. Case Studies

A. Modified WSCC Three-Machine-Nine-Bus Test Power Grid

We employ a commonly used nine-bus power system to test and compare the performance of various inertial control methods. Each generator is equipped with an excitation and governor to control the terminal voltage and system frequency in the model. We modify the original one to facilitate the test as shown in Fig. 6, in which a small generator, SG4, is connected to BUS 7 to trigger the frequency event. The aggregated WPP, including a certain amount of identical wind turbines, is connected at BUS 4. The parameters of the simulated system can be found in [16] and [19].

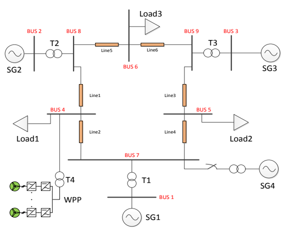

Figure 6. Modified WSCC 9-bus power system

To emulate the actual frequency response of a power system, the automatic generation control (AGC) is also included in the modeled test system. The AGC is simplified using proportional-integral controllers in this isolated power system. The AGC is slower than the droop-based primary frequency response, which can be realized by tuning the integration gain K_i of the proportional-integral control.

B. Stage 1: Assessing the Inertial Response in Simulink Using FAST and TurbSim

Taking advantage of the powerful simulation tools developed by the National Renewable Energy Laboratory, the inertial control methods are assessed and compared under highly turbulent wind conditions. We connect the FAST-based CART3 model to the test power system simulated in Simulink. The wind speed profile with different turbulent intensities (TI) are generated using TurbSim. Besides the electric power and rotor speed data of the CART3, the mechanical variables, such as the bending moments on the tower and blades, are collected.

The inertial control methods, FBIC and TLIC, are compared with the baseline control method. As the turbulent intensities are set to 5% and 10% in the two cases, it is obvious that the wind speed profile is more turbulent with the higher TI value on the left column of Fig. 7. For the FBIC method, we employ the measures in [20] to determine the scale factors for the derivative and deviation terms.

According to Fig. 7(c), the rotor speed recovers successfully after the kinetic energy is released under the highly turbulent wind conditions. Compared to the active power boost provided by the WPP, the CART3 discharges more power to support the grid frequency using the TLIC method as shown in Fig. 7(b). The active power boost of the CART3 is faster and stronger with the TLIC method. As a result, the frequency nadir (FN) is improved much more than the FBIC method. However, the TLIC method extracts the kinetic energy by regulating the wind turbine close to its overproduction limit, so the rotor speed decelerates more in both cases, and it takes longer to restore the kinetic energy in the rotating mass. In addition, a larger power decrease tends to accelerate the rotor speed faster; however, a second frequency dip may be observed. As presented in Fig. 7(d), small second frequency dip happens in the scenarios with the TLIC method; by contrast, the grid frequency recovers to the nominal value smoothly in the scenarios with the FBIC method. This recovery is because the WPP with the FBIC method regulates the grid frequency in coordination with other resources in the grid, which is the same as the droop-based distributed control in a microgrid through the frequency measurement [21], so the frequency oscillation can be damped in this case. A stronger frequency regulation is observed with the TLIC method and the WPP regulates the grid frequency without coordinating with other resources in the grid. The frequency overshot above the nominal value and secondary frequency dip may be observed. The second frequency dip may be rather severe, especially when the WTG begins to restore the kinetic energy by decreasing its power output when the initial frequency dip is not fully arrested [22].

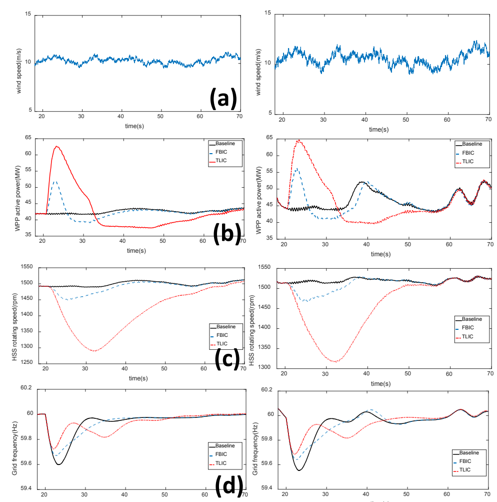

Figure 7. The performance of the CART3 with FBIC and TLIC methods under different wind turbulent intensities: (a) wind speed profile, (b) WPP active power output, (c) high-speed-shaft rotating speed, and (d) grid frequency (left column: 5% turbulence intensity (TI), right column 10% TI)

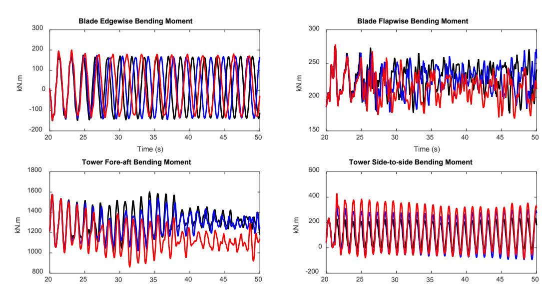

Figure 8. The impact of inertial control on the wind turbine mechanical components (black line: baseline control, red line: TLIC, blue line: FBIC)

The impact of the inertial control methods on the wind turbine mechanical components are examined in the simulation. According to Fig. 8, the inertial response increases the side-to-side bending moment of the tower, and the blade edgewise bending moment remains almost the same with the inertial response. In contrast, the inertial response can reduce the loads on the flapwise of the blade, as well as the tower fore-aft bending moment. This may be because the wind turbine is operated with a suboptimal power coefficient when the inertial response is released. In this situation, the loads on the wind turbine components are mitigated by letting more wind pass through the turbine blades, so the thrust force of wind is reduced.

C. Stage 2: Assessing the Inertial Response of the CART3 Using HIL Techniques

In this part of the study, the HIL techniques are employed to test the inertial response of the real CART3. The proposed control algorithms are compiled to a dynamic link library file in Simulink, which can be embedded into the CART3 SCADA system to control the real wind turbine. By doing so, the wind turbine control strategies can be designed and tuned effectively, thereby taking advantage of the code transformation between Matlab and LabVIEW.

Note that the CART3 only exchanges signals with the modeled power system in RTDS, and no power amplifier is required in this simulation. The stability of the closed-loop simulation can be ensured because the time delay and distortion generated by the A/D (D/A) conversion can be neglected compared to that introduced by the power amplifier in the power-hardware-in-the-loop scenario [23].

By manually triggering the frequency event in the simulated power system, the response of the wind turbine is documented. Fig. 9 shows the inertial response of the CART3 activated with FBIC and TLIC, respectively. According to the figures, the CART3 increased its active power output when the frequency excursion was detected. It is impressive that the increased active power can be up to 30%–50% of the predisturbance power level. The rotor speed is recovered gradually after the inertial response is terminated.

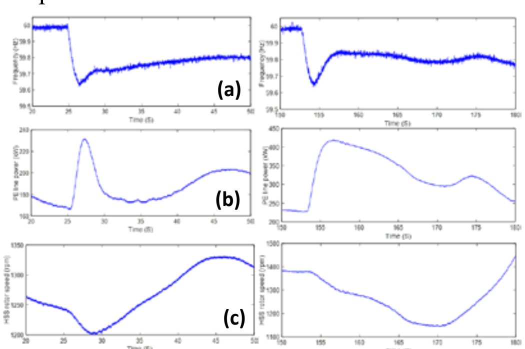

Figure 9. The CART3 inertial response using the FBIC method (left column) and TLIC method (right column): (a) grid frequency, (b) power electronics line power, and (c) high-speed-shaft (HSS) rotating speed

V. Conclusion

The inertial response of a variable-speed wind turbine is evaluated in this paper. A two-stage simulation platform was developed, which combines the offline simulation and real-time simulation, and takes advantage of the code transformation interface between Matlab/Simulink and LabVIEW. The simulation results provide insights into the design of the inertial response with two distinct inertial control methods, each of which present different features for the frequency support. At last, the inertial response of the CART is verified in the HIL simulation, in which the real turbine is operated against the virtual power system modeled in RTDS. The experimental results show the great potential of wind turbines participating in grid frequency regulation.

VI. References

[1] E. Ela, V. Gevorgian et al., "Active power controls from wind power: Bridging the gap," National Renewable Energy Laboratory, Golden, CO, Tech. Rep., 2014.

[2] P. W. Carlin et al., "The history and state of the art of variable-speed wind turbine technology," *Wind Energy*, vol. 6, no. 6, pp. 129–159, 2003.

[3] M. Altin, et al., "Methodology for assessment of inertial response from wind power plants," in *Proc. 2012 Power and Energy Society General Meeting*.

[4] M. Kang, et al., "Frequency Control Support of a Doubly-Fed Induction Generator Based on the Torque Limit," *IEEE Trans. Power Syst*., to be published.

[5] J. F. Conroy, W. Rick, "Frequency response capability of full converter wind turbine generators in comparison to conventional generation." *IEEE transactions on power systems*, vol. 23, no. 2, pp. 649-656, 2008.

[6] J. Morren, J. Pierik, and S. W. H. De Haan, "Inertial response of variable speed wind turbines," *Electric Power Systems Research*, vol. 76, no. 11, pp. 980–987, 2006.

[7] Mauricio, J. M., et al. "Frequency regulation contribution through variable-speed wind energy conversion systems." *IEEE Transactions on Power Systems*, vol 24, no. 1, pp. 173-180, 2006.

[8] N. R. Ullah, T. Thiringer, and D. Karlsson, "Temporary primary frequency control support by variable speed wind turbines—potential and applications," *IEEE Trans. Power Syst*., vol. 23, no. 2, pp. 601–602, 2008.

[9] Samer U., El I., D. Annakkage, and Geza Joos., "Short-term frequency support utilizing inertial response of DFIG wind turbines," in *Proc. 2011 Power and Energy Society General Meeting*.

[10] J. M. Jonkman and M. L. Buhl, "FAST user's guide," National Renewable Energy Laboratory, Golden, CO, NREL/EL-500-29798, 2005

[11] B. Jonkman, "Turbsim user's guide: Version 1.50," National Renewable Energy Laboratory, Golden, CO, USA, Tech. Rep. NREL TP-500-46198, Sep. 2009.

[12] E. Muljadi et al., "Understanding inertial and frequency response of wind power plants," in *Proc. 2012 IEEE Power Electronics and Machines in Wind Applications*.

[13] E. Muljadi, and P. B. Charles. "Pitch-controlled variable-speed wind turbine generation." *IEEE Transactions on Industry Applications,* vol. 37, no. 1, pp. 240-246, 2001.

[14] B. Wu, et al., *Power conversion and control of wind energy systems*. New York: John Wiley & Sons, 2011.

[15] P. A. Fleming, J. Aho, A. Buckspan et al., "Effects of power reserve control on wind turbine structural loading," *Wind Energy*, vol. 17, no. 3, pp. 453-469, 2015.

[16] Z. Wu, W. Gao and X. Wang, et al. "Improved Inertial Control for permanent magnet synchronous generator wind turbine generators." *IET Renewable Power Generation*, to be published.

[17] J. H. Jeon, et al. "Development of hardware in-the-loop simulation system for testing operation and control functions of microgrid." *IEEE Transactions on Power Electronics*, vol. 25, no. 12, pp. 2919-2929, 2010

[18] M. Hwang, et al., "Dynamic Droop-Based Inertial Control of a Doubly-Fed Induction Generator," *IEEE Trans. Sustainable Energy*, to be published.

[19] X. Wang, W. Gao, and J. Wang et al. in *Proc. 2016 North America Power Symposium*, to be published.

[20] Z. Zhang, Y. Sun, J. Lin, and G. Li, "Coordinated frequency regulation by doubly fed induction generator-based wind power plants," *IET Renew. Power Gen*., vol.6, no.1, pp.38-47, Jan. 2012.

[21] N. Pogaku, P. Milan, and C. G. Timothy. "Modeling, analysis and testing of autonomous operation of an inverter-based microgrid." *IEEE Transactions on power electronics*, vol. 22, no. 2, pp. 613-625, 2007.

[22] Eto, J. H. "Use of frequency response metrics to assess the planning and operating requirements for reliable integration of variable renewable generation." Lawrence Berkeley National Laboratory (2011).

[23] W. Ren, M. Steurer, and T. L. Baldwin. "Improve the stability and the accuracy of power hardware-in-the-loop simulation by selecting appropriate interface algorithms." *IEEE Transactions on Industry Applications*, vol. 44, no. 4, pp. 1286-1294, 2008.